A multi-metric assessment of drought vulnerability across different vegetation types using high resolution remote sensing

Chen, Q.; Timmermans, J.; Wen, W.; Bodegom, P.M. van

A multi-metric assessment of drought vulnerability across different vegetation types using high resolution remote sensing

Qi Chen [a,*], Joris Timmermans [a,b,c], Wen Wen [a], Peter M. van Bodegom [a]

[a] Institute of Environmental Sciences (CML), Leiden University, 9518, 2300 RA Leiden, the Netherlands
[b] Virtual Laboratory and Innovation Centre (VLIC), Lifewatch ERIC, Science Park 904, 1098 XH Amsterdam, the Netherlands
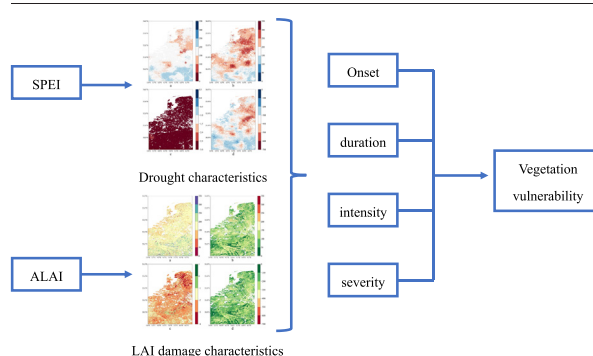[c] Institute for Biodiversity and Ecosystem Dynamics (IBED), University of Amsterdam, 1090 GE Amsterdam, the Netherlands

HIGHLIGHTS

- A new framework based on drought and vegetation impact characteristics is proposed.
- High resolution estimates of drought and drought damage were derived from remote sensing.
- Vulnerability was comprehensively assessed by multiple internally consistent metrics.
- Mosaic grasslands and tree croplands were most vulnerable to the 2018-drought.
- Our framework shows multi-faceted strategies of different vegetation types to drought.

GRAPHICAL ABSTRACT

ARTICLE INFO

ABSTRACT

Drought impact monitoring is of crucial importance in light of climate change. However, we lack an understanding of the concomitant responses of ecosystems to a variety of drought characteristics and the links between drought and ecosystem anomaly characteristics for a comprehensive set of vegetation types to provide needed information for water management. In response, this study presents a new framework that allows us to explore the relationship between drought and its impact on ecosystems in greater detail. Specifically, our framework focuses on estimating jointly the hydrological and ecosystem temporal evolution and anomalies around a drought event using four pairs of metrics: onset-onset, duration-duration, intensity-intensity, and severity-severity of drought and vegetation damage. Additionally, we incorporated a metric on vegetation vulnerability based on changes in damage severity along a gradient of increasing drought severity. Based on this framework, we evaluated drought vulnerability patterns of various vegetation types across the Netherlands and Belgium in 2018 at high spatiotemporal resolution. Our results reveal a differential vulnerability of vegetation between ecosystems with increasing drought severity, which could aid future drought impact predictions. In particular, mosaic grasslands and tree/shrub croplands are highly sensitive to increasing drought severity. Individual characteristics (onset, duration, intensity and severity) of drought and vegetation damage behave differently in various vegetation types. For instance, broadleaved forests respond faster than other forests, while mixed forests suffer less damage than other types. The early warning threshold to drought for most vegetation types is around a Standardized Precipitation Evapotranspiration Index (SPEI) value of −1. The characterization of a suite of drought response characteristics through our impact analysis framework can be used in a wide variety of regions to understand current and possible future responses to drought.

* Corresponding author.
  E-mail addresses: q.chen@cml.leidenuniv.nl (Q. Chen), j.timmermans@cml.leidenuniv.nl (J. Timmermans), w.wen@cml.leidenuniv.nl (W. Wen), p.m.van.bodegom@cml.leidenuniv.nl (P.M. van Bodegom).

1. Introduction

The frequency of droughts in Europe has increased over the past decades (Briffa et al., 2009) (Vicente-Serrano et al., 2014). With ongoing global climate change, droughts are predicted to become even more frequent and more intense in many regions of Europe (Spinoni et al., 2018) (Ruosteenoja et al., 2018)(Grillakis, 2019). These natural disasters may severely impact the stability of multiple ecosystems (Ciais et al., 2005) (Semenov and Shewry, 2011)(Saatchi et al., 2013), and consequently their associated ecosystem services.

To reduce the impact of such droughts, water needs to be allocated to both natural and agricultural ecosystems during drought. To govern the allocation of water, policy makers do not only need knowledge of water stress itself but also a clear understanding of the vulnerability of different vegetation types, so as to protect ecosystems most at risk. Water management thus demands answering questions regarding i) which vegetation types are more sensitive to water stress, ii) when will vegetation be impacted, and iii) what will be the damage? Thus, a multi-metric quantitative analysis of drought vulnerability of vegetation, which includes these three aspects, is of great significance for water management.

Unfortunately, present-day drought impact monitoring frameworks lack this capability, and only answer the first aspect. Various indices exist to quantify the severity of meteorological drought, such as the Standardized Precipitation Index (SPI) (McKee et al., 1993), the Palmer drought severity index (PDSI) (Palmer, 1965) and the standardized precipitation evapotranspiration index (SPEI) (Vicente-Serrano et al., 2010). Likewise, to identify ecosystem health, multiple vegetation indices have been constructed to capture the vegetation growth and status, such as the Normalized Difference Vegetation Index (NDVI), the Vegetation Condition Index (VCI) (Kogan, 1995a), the Vegetation Health Index (VHI) (Kogan, 1995b) (Kogan, 1997), and the Enhanced Vegetation Index (EVI) (Huete et al., 2002). By correlating drought indices (e.g., SPEI, PDSI, and SPI) with vegetation indices (e.g., NDVI), previous studies evaluated vegetation responses to drought in the Mediterranean region (Gouveia et al., 2017), China (Ding et al., 2020) and the Northern great plains (Ji and Peters, 2003) across different vegetation types (Zhang et al., 2017)(Zhao et al., 2018)(Páscoa et al., 2018). These studies quantified which vegetation types are more sensitive to drought (i.e. the first question identified above), but are limited in advancing our understanding of how much the vegetation will be impacted and when will be the start of this vegetation damage.

A multi-metric framework that quantifies all three aspects in the relationship between vegetation responses and drought can build on drought characterization studies that identified drought onset, duration, intensity and severity to better quantify drought evolution (Mishra and Singh, 2010)(Gebremeskel Haile et al., 2020)(Yao et al., 2020)(Chiang et al., 2021). Previous studies have applied these metrics to evaluate agricultural drought (Brito et al., 2018), but applications comparing responses between vegetation types are missing.

In addition, a comprehensive investigation of the linkage between drought characteristics and multiple vegetation damage characteristics is missing. This hampers a full evaluation of vegetation responses to drought which are likely to be multi-faceted, given that different plant species or functional groups have different strategies to cope with drought (Larcher, 2003)(Volaire, 2018)(Forner et al., 2018). Current research might thus have missed particular drought responses of vegetation in general and certain vegetation types in particular. This research gap limits the accurate prediction of future vegetation damage and ecosystems' responses to the forecasted drought intensification (Field et al., 2012)(Choat et al., 2012). Specifically, it remains unknown how vegetation vulnerability changes along with increasing drought severity and how this change varies between vegetation types. Such insights will be instrumental to making predictions of future damage and provide an early warning signal to drought impacts. Thresholds in vegetation responses are also important in this respect (Brown, 2008)(Sepulcre-Canto et al., 2012).

Such comprehensive vulnerability assessments of ecosystems can only be achieved when taking the high spatial heterogeneity of vegetation types into account (Vicente-Serrano et al., 2013), and by distinguishing the variety of plant strategies to deal with drought (Fang and Xiong, 2015). Traditional remote sensing drought monitoring products lack such high spatio-temporal resolutions. For instance, there is no daily SPEI product at high spatial resolution. Instead, for the calculation of SPEI, precipitation data used by most pan-European studies is limited to a coarse resolution (>25 km) (Sun et al., 2018). Likewise, the temporal scale has been relatively coarse with the majority of studies calculating SPEI on monthly time scales (Bachmair et al., 2018)(Rita et al., 2020). Considering the high spatial heterogeneity in vegetation type occurrences and their differences in response to drought, such spatiotemporal resolutions are not sufficient to accurately quantify the vulnerability of vegetation.

The aim of this research is to deal with the research gaps identified above by quantitatively analyzing drought vulnerability across different vegetation types using a series of internally consistent drought and vegetation damage characteristics simultaneously based on high-resolution data. To achieve this aim, we built a framework identifying the onset, duration, intensity and severity of drought and its corresponding vegetation anomalies. In particular, the framework should allow us to answer the following research questions: What are the characteristics of vegetation anomaly events? Do individual vegetation characteristics respond differently to drought metrics? How does vulnerability vary between vegetation types with changing drought severity? What is the early warning threshold of drought for vegetation damage?

To evaluate our framework, we utilize the 2018 summer drought in the Netherlands and Belgium (Philip et al., 2020)(Buitink et al., 2020). This 2018 drought event was climatically more extreme than previous events. It therefore provides a very suitable event for evaluating our framework on drought impacts. Leaf area index (LAI) was used as an indicator of vegetation responses in our analysis. LAI is more representative of vegetation structure and functioning compared to indices like NDVI, EVI, and VCI (Gower and Norman, 1991)(Garrigues et al., 2006). Also, LAI is a key parameter within land surface models due to its impact on energy transfer between the canopy and the atmosphere (Chen et al., 1997)(Tang et al., 2014). A better understanding of LAI responses to water stress can deepen the understanding of the impact of drought on entire ecosystem processes.

In combination, our framework will allow making valuable predictions on the vegetation vulnerability for upcoming droughts. Our methodology distinguishes itself from previous studies through a) building quantitative relationships between drought characteristics and drought impacts by multiple internally consistent characteristics (onset, duration, intensity, and severity) of both drought and vegetation anomaly events, b) the analysis of drought vulnerability, defined as the changes in vegetation damage with drought severity, across a wide suite of vegetation types, c) providing an early warning threshold for drought damage of vegetation, and d) its much higher spatial and temporal resolution of the remote sensing products.

2. Materials and methods

2.1. Data sources and preprocessing

In this study, we used the SPEI drought index (calculated from long-term precipitation and evapotranspiration data) to quantify drought and calculated the anomalies of LAI (ALAI) to identify the impact of the event. Next, we estimated the onset, duration, peak intensity, severity of drought and ALAI, and compared them for different vegetation types. The technical roadmap of the new framework to analyze the vegetation vulnerability is shown in Fig. 1.

2.1.1. Precipitation data

Two datasets (from remote sensing and ground observations) were fused together for 2004 to 2018 to combine the advantages of each product. Remote sensing products provide a wide coverage and high time resolution,
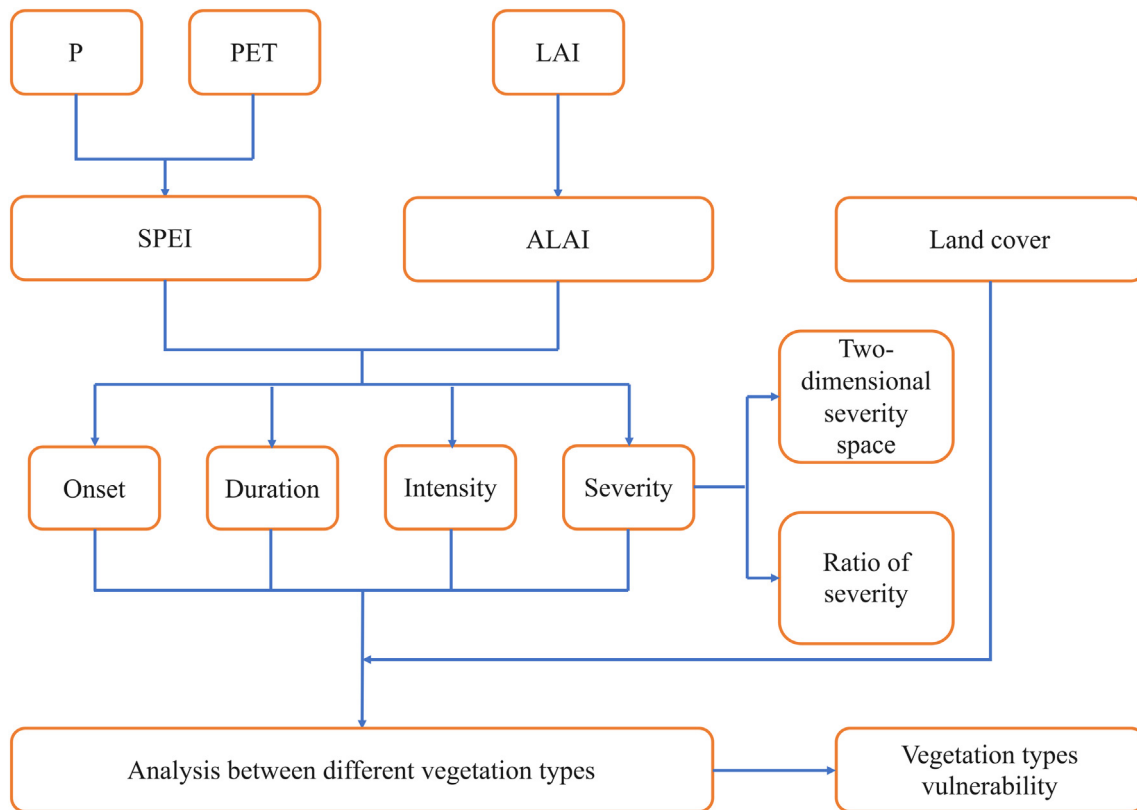
Fig. 1. Technical roadmap of the new framework. P represents precipitation, PET represents potential evapotranspiration, LAI represents leaf area index, SPEI represents standardized precipitation evapotranspiration index, ALAI represents anomaly LAI.

while ground measurements are deemed to have a higher accuracy. By combining these two we extract the best of both worlds, allowing for a more detailed analysis of drought conditions and impacts. The processing details are in supplementary Fig. S1.

The remote sensing precipitation data was acquired using the Spinning Enhanced Visible and Infrared Imager (SEVIRI) on board of Meteosat Second Generation (MSG) operated by EUMETSAT. The SEVIRI instrument scans the complete Earth every 15 min. Over northern Europe (including the Netherlands) the satellite viewing zenith angle of SEVIRI is about 60°, and has a spatial resolution of about 4×7 km^2 (Roebeling and Holleman, 2009). We used the data product developed by the Royal Dutch Meteorology Institute (KNMI) (https://msgcpp.knmi.nl/), which retrieved precipitation data from cloud physical properties as derived from the original SEVIRI measurements (Roebeling et al., 2006). The dataset covers the time period 1 January 2004 – present.

In order to improve upon the accuracy of the remote sensing precipitation product, we integrated it with the daily Meteorological dataset from the Agri4Cast Data portal of the Joint Research Center (JRC) (Toreti, 2014). This dataset consists of 25 km × 25 km grid cells interpolated from weather station observations. The temporal coverage of the datasets is from 1979 to the last complete calendar year and the spatial coverage includes the European Union and neighboring countries.

2.1.2. PET data

The MOD16A2 Version 6 from the Moderate Resolution Imaging Spectroradiometer (MODIS) sensor aboard the Terra platform was used to get potential evapotranspiration (PET) estimates (Running et al., 2017). This product is an 8-day composite dataset produced at 0.5 km spatial resolution. To obtain daily estimates, we resampled this dataset to daily values. Its temporal extent is 2001 to present.

2.1.3. LAI data

To evaluate variations of vegetation patterns during drought, the Copernicus Global Land Service GEOV2 Leaf Area Index (LAI) was used at 1 km resolution (Copernicus Service Information, 2022). GEOV1 outperforms other existing global products in terms of accuracy and precision (Camacho et al., 2013). GEOV2 aims to improve GEOV1 in terms of continuity while being consistent with GEOV1 in terms of accuracy (Verger et al., 2014). GEOV LAI has been demonstrated to show a smoother seasonal trajectory than MODIS data. The LAI 1 km product is a global 10-days product that spans from 1999 to present.

2.1.4. Vegetation type data

The land cover product at 300 m spatial resolution on an annual basis provided by Copernicus Climate Change Service (C3S) was used to identify different vegetation types (C3S, 2019), consistent with the series of global land cover maps from 1992 to 2015 produced by the European Space Agency (ESA) Climate Change Initiative. The 2018 land cover map was used in this study (Fig. 2; Table 1).

To match the rainfall data with the evapotranspiration data, and to retain the data accuracy of evapotranspiration to the greatest extent, thereby reducing data loss, we resampled all datasets into a grid of 0.005 degrees (around 0.5 km) under the World Geodetic System 84 (WGS84) coordinate system by using python package GDAL and executed all analyses based on this grid.

2.2. Analysis

2.2.1. Drought and drought characteristics index

SPEI is based on the climatic water balance between precipitation and PET, and can be calculated at different time scales to facilitate multiscalar drought assessment (Vicente-Serrano et al., 2010). Based on the fused high-resolution precipitation data and PET data, we calculated the
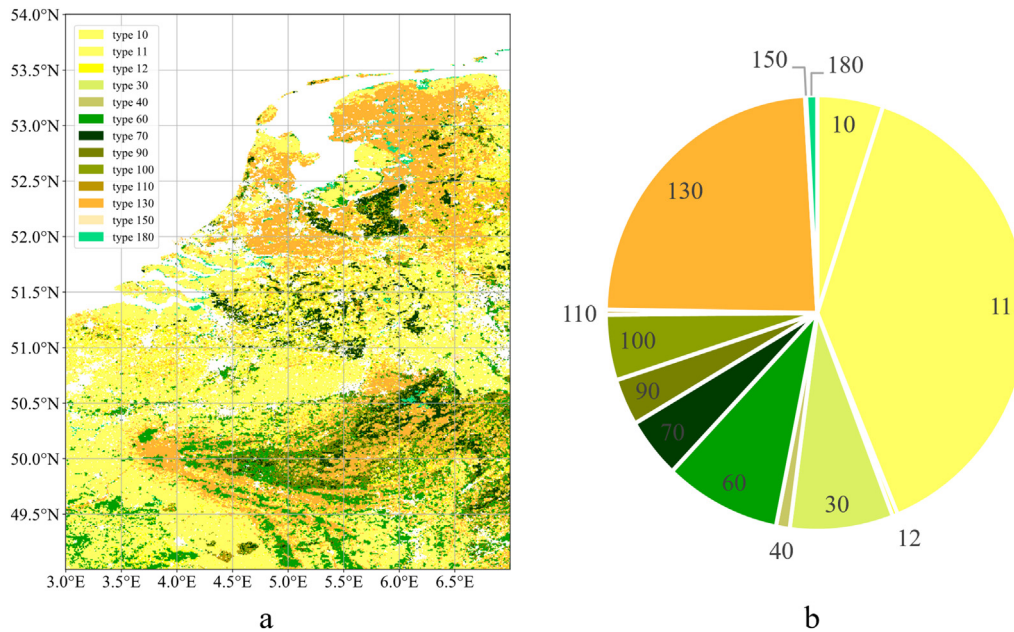

Fig. 2. a) land cover map, in which the vegetation types represented are coded according to Table 1. b) The proportion of each vegetation type in the study area.

daily SPEI for 2018. Our Python code to calculate SPEI was obtained from the U.S. drought portal (www.drought.gov) (Adams, 2017). On the basis of this code, we changed the original SPEI calculation time step from monthly to daily. The daily SPEI calculation process is similar to that of monthly SPEI (Wang et al., 2015)(Vicente-Serrano et al., 2010).

We chose 1, 2, 3, 4, 5 and 6 months as our SPEI time scales to have a full range of possible responses. 3-month time scale SPEI has been demonstrated to be the optimal time scale to investigate the response of European vegetation to drought (Ivits et al., 2016). To evaluate if this also applied to our study area, we determined the correlation between the daily standardized anomaly LAI (SALAI, discussed in Section 2.2.2) and daily SPEI for each pixel. The maximum Pearson correlation coefficient between SALAI and SPEI and the corresponding time scale was extracted for each pixel. Since most of the pixels showed a significant relation, we removed those pixels that did not show a significant correlation. Based on this analysis, we confirmed that 3-month SPEI has a generally good correlation with vegetation responses in different vegetation types (supplementary Fig. S2). Therefore, we selected SPEI on a 3-month time scale for our subsequent analyses (See Fig. S3 for the spatial patterns of the correlation between SPEI and SALAI).

To comprehensively describe the distribution of drought in 2018, we calculated the start date, duration, peak intensity, and severity of SPEI as indicators. Following (Jamro et al., 2020) (McKee et al., 1993), we defined

SPEI = −0.5 as the threshold to indicate the onset of drought. We first selected all SPEI values lower than −0.5 in 2018, then selected the longest drought event, and calculated the start date of the longest drought event. For drought duration, the number of days with a SPEI less than −0.5 in 2018 was used. The minimum value reached by SPEI in 2018 was set as drought peak intensity. The sum of all SPEI values less than −0.5 in 2018 represents the drought severity in 2018.

2.2.2. LAI anomaly and LAI responses

In order to evaluate responses of different vegetation types to the drought event of 2018, we calculated the anomalies of LAI between 2018 and the LAI of the prior fifteen years (2004–2018). We calculated the Standardized Anomaly LAI (SALAI) by using Eq. (1):

$$SALAI(t) = \frac{LAI(t) - \overline{LAI}(t)}{\sigma(t)} \tag{1}$$

where $SALAI(t)$ is the SALAI at time t, $LAI(t)$ is the LAI value for time t, $\overline{LAI}$ is the mean LAI at time t over 15 years, and σ is the standard deviation of the mean LAI over 15 years. Our calculation is based on the 10-days temporal resolution of the original LAI data, after which we interpolated this result to daily data.

Table 1

Vegetation types included in this study, as classified by the European Space Agency (ESA) climate change initiative.

Global	Regional*	Vegetation type	# pixels
10		Cropland, rainfed	25,457
	11	Cropland, rainfed, herbaceous cover	196,096
	12	Cropland, rainfed, tree or shrub cover	1974
30		Mosaic cropland (>50%) /natural vegetation (tree, shrub, herbaceous cover) (<50%)	39,982
40		Mosaic natural vegetation (tree, shrub, herbaceous cover) (>50%) /cropland (<50%)	5298
60		Tree cover, broadleaved, deciduous, closed to open (>15%)	45,100
70		Tree cover, needleleaved, closed to open (>15%)	22,720
90		Tree cover, mixed leaf type (broadleaved and needleleaved)	17,532
100		Mosaic tree and shrub (>50%) /herbaceous cover (<50%)	24,620
110		Mosaic herbaceous cover (>50%) /tree and shrub (<50%)	1896
130		Grassland	120,482
150		Sparse vegetation (tree, shrub, herbaceous cover) (<15%)	437
180		Shrub or herbaceous cover, flooded, fresh/saline/brakish water	4280

* Cropland 10 is the definition of crops at the global level, and 11 and 12 are definitions at the regional level, subdividing croplands.

To understand LAI responses, we used the same indicators as for drought. Based on the analogy in calculations of SALAI and SPEI, we calculated the onset date, duration, peak intensity, and severity of the anomaly LAI (ALAI). The calculation method of these indices is the same as for drought, except that we set the LAI anomaly threshold to −1. The lower threshold for LAI was chosen to reduce the risk of non-drought related events to be included. Based on the longest LAI anomaly, the number of days between its onset date and when it reaches the minimum ALAI value was set as a decline period (supplementary Fig. S4). For croplands, the only vegetation type with annual (instead of perennial) plants, only drought impacts during the growing season were included. For our study area, the growing seasons start around mid-May (Khabbazan et al., 2019) till November.

2.2.3. Drought-vegetation damage relationships

We compared the onset, duration, peak intensity, severity of drought and ALAI in different vegetation types. For onset and duration, pixel-based differences between drought and ALAI were determined, evaluating delays and duration differences in drought impacts through a one-sample t-test against zero. Given the difference in units, this was not possible for severity and intensity and unequal variance independent t-tests were used instead. To explore vulnerability across different vegetation types with a changing drought severity, we made contour plots of drought severity vs. ALAI severity for each vegetation type, based on the density of points as calculated from Gaussian kernel density estimations. We took the ratio of ALAI severity and drought severity as an additional measure of vulnerability. Since ratios can show extreme maximum values, we removed outliers larger than the 99.9th percentile of the data. Finally, to evaluate the drought conditions that trigger ALAI, we extracted the SPEI value corresponding to the start date of the longest LAI anomaly.

3. Results

3.1. 2018 drought response of different vegetation characteristics

Fig. 3 shows the spatial distribution of drought response characteristics based on high-resolution ALAI data. Anomalies in LAI appeared earlier in the northern and western coastal regions. The LAI of regions in southeastern Belgium and northern France responded later than northern regions, and some forests in this area were not affected at all. The duration of ALAI was long in the western parts of Belgium, the Netherlands, and Germany, while the LAI in some inland areas of the Netherlands, such as the Veluwe, was only affected for a short time (Fig. 3b), despite experiencing a long period of drought (Fig. S5b). The southern forests in Belgium, northern France, and Germany were also affected for a short time only. The northeastern part of the Netherlands showed the strongest drought intensity, while the northwestern part of France only reached a mild drought intensity (Fig. 3c). LAI anomaly severity patterns (Fig. 3d) were very similar to the duration pattern. These LAI responses seemed closely related to vegetation type, which is further explored in the next section.

3.2. Individual characteristics behave differently in drought response

By quantifying the same characteristics (onset, duration, intensity and severity) of drought and anomaly LAI events, the relationships in individual characteristics between drought and drought impact were assessed to create a comprehensive understanding of drought impacts. The patterns in onset, duration, intensity, and severity of drought vs. the corresponding vegetation responses are shown in Fig. 4.

Vegetation responses to drought are delayed to different extents in different vegetation types. As shown in Fig. 4a, in general, the onset of ALAI was later than that of the longest drought event. The exception to this pattern is sparse vegetation, showing an earlier start than the longest drought event. This may be due to generally low LAI of this landcover type, which makes detecting anomalies in LAI more uncertain. Moreover, short drought events occurred prior to the longest drought event and may have induced

vegetation damage. Herbaceous croplands and tree/shrub croplands showed a very short delay time, which indicates that these vegetation types are more sensitive to drought. The onset of vegetation impacts in forests had a relatively long delay compared to other vegetation types. Especially, needleleaved forests and mixed forests showed a long delay, indicating that they have a certain degree of drought resistance. These two forests also showed lower correlation coefficients between SPEI and SALAI (Fig. S3). Tree/shrub croplands reacted quickly and had higher correlation coefficients.

The length of the vegetation damage period also links differently to drought duration in various vegetation types. Fig. 4b shows that the duration of damage of all vegetation types was generally shorter than the actual drought. However, broadleaved deciduous forests, needleleaved forests and mixed forests were affected for a relatively shorter time (corresponding to stronger differences in duration) than other vegetation types, with up to 4–5 months shorter durations of impacts. Sparse vegetation and wetland vegetation also showed shorter durations of drought impacts (i.e. large differences in duration). Grasslands and croplands, on the other hand, suffered a long drought impact period (i.e. a small difference in duration).

The drought peak intensity of all vegetation types reached the most intense conditions of SPEI = −3.0 (Fig. 4c). The ALAI peak intensity in grasslands was most severe, while the peak intensity reached less intense values in broadleaved deciduous forests, needleleaved forests, mixed forests, and sparse vegetation. All crops showed similar damage intensity.

The pattern of severity (Fig. 4d) is consistent with the result of drought duration and its variation between vegetation types. The severity of the 2018 drought in broadleaved deciduous forests and mixed forests was relatively low. The drought severity in tree/shrub croplands was similar to that of broadleaved deciduous forests, while tree/shrub croplands suffered much more damage. Needleleaved forests seem to grow in areas with high drought severities.

3.3. Vulnerability of vegetation types to drought

To help building predictions of how an increasing drought severity in the future could impact ecosystems, we explored vegetation vulnerability.

The contour patterns between ALAI severity and drought severity provide a new view on evaluating the vulnerability of vegetation to drought. Fig. 5 shows that broadleaved deciduous forests, needleleaved forests and mixed forests showed low vegetation damage for a wide range of drought severities. There was variation in vulnerability within these vegetation types, possibly due to differences in local conditions. Other vegetation types, such as agricultural types, were more sensitive to drought than forests. Especially for tree/shrub croplands, vegetation was already seriously damaged when drought was not that severe, indicating that these systems (in the Netherlands mainly consisting of orchards) are relatively fragile. Also grasslands were relatively fragile. Mosaic grasslands showed a very clear response pattern: as the severity of drought increased, the damage to the vegetation also increased. Intriguingly, such patterns were much weaker in most of other vegetation types, suggesting that –apart from clear differences in overall vulnerability – local conditions determine the actual vulnerability. This assessment based on drought severity – vegetation impact severity provides a description of vulnerabilities for different vegetation types facing increasing drought stress (Fig. S6), and gives an opportunity to build predictions of how much the vegetation will be damaged when suffering future drought events.

The ratio of ALAI severity to drought severity (Fig. 6) provides another measure of vulnerability, indicating the vegetation damage per unit drought. Trees tend to take up soil moisture from deeper layers than grasslands and crops, which may explain why forests showed relatively lower vulnerability than other vegetation types. Broadleaved deciduous forests, and needleleaved forests showed similar vulnerability, while mixed forests seemed to be the least vulnerable (expressed as a low severity ratio). Mosaic forests were the most vulnerable of all forested vegetation types, likely due to the mixing with shrub and herbaceous cover. Among agricultural land, tree/shrub croplands showed the highest severity ratio (mean 0.77),
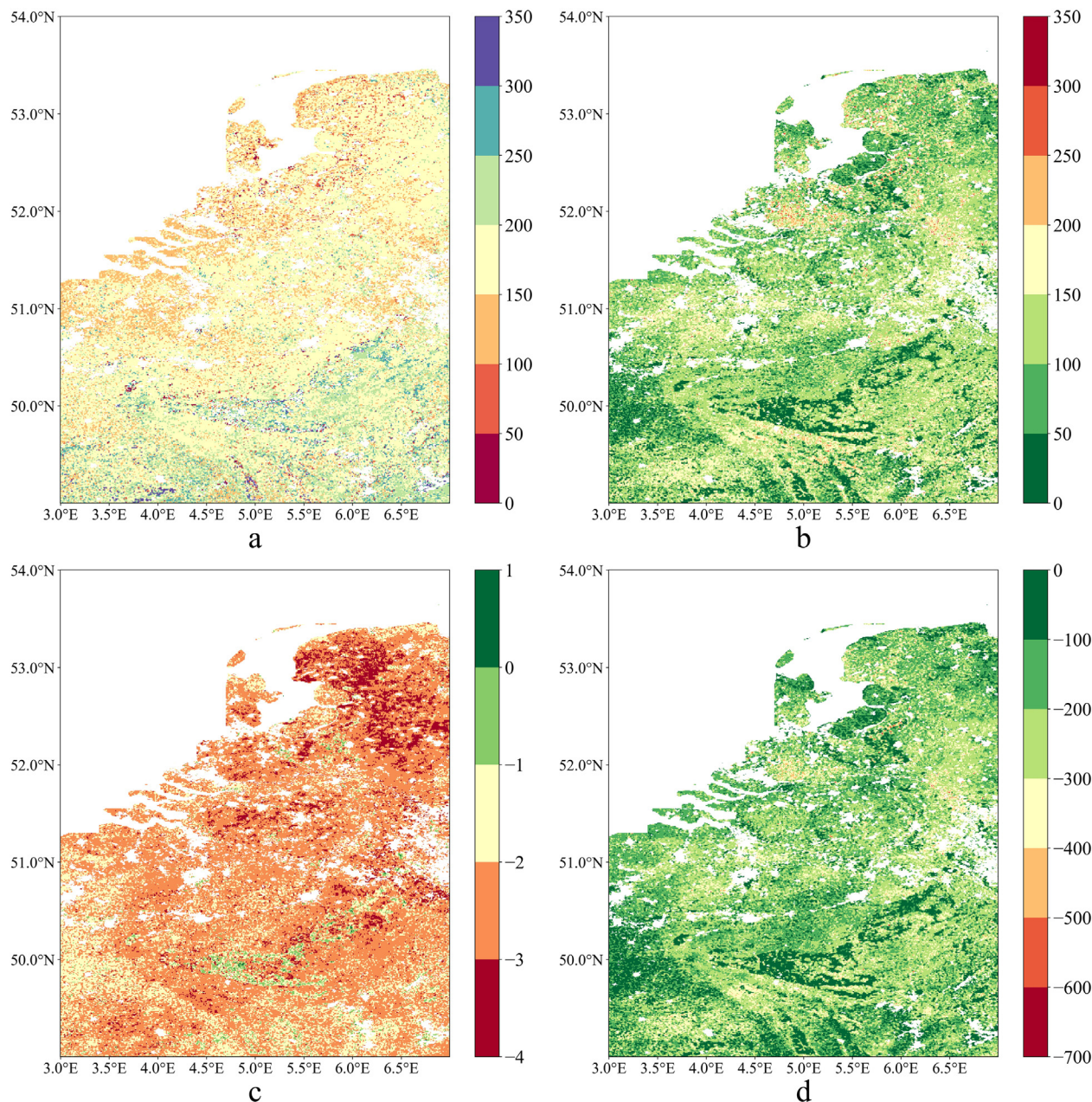
Fig. 3. Spatial-temporal drought impacts on vegetation. Panels a-d show onset, duration, max-intensity, and severity of anomaly LAI (ALAI), respectively.

indicating that tree/shrub crops seem to be more vulnerable than herbaceous crops. The vulnerability of grasslands was higher than for all forest vegetation types and higher than for all croplands other than tree/shrub croplands. The vulnerability of sparse vegetation and wetland vegetation was low. For sparse vegetation, the pattern may have been affected by its low LAI values which made detecting its variation inaccurate. The environment of wetland vegetation is relatively moist, and may therefore be less affected by drought.

3.4. Early warning threshold of drought for the damage of vegetation

The SPEI value at the onset of anomaly LAI event (Fig. 7) provides an early warning signal of drought impacts, indicating the drought conditions at which a vegetation anomaly would be triggered.

Onsets in LAI anomaly started at mild SPEI values in tree/shrub croplands and herbaceous croplands. Tree/shrub croplands anomalies started at SPEI values around −0.5, and herbaceous croplands anomalies started

at SPEI values greater than −1. Compared with other terrestrial vegetation types, the LAI anomalies occurred under more intense drought conditions in forests, especially for needleleaved forests whose mean was even lower than that of wetland vegetation. For mixed forests, the LAI anomaly started at a relatively intense drought, and a large part of the broadleaved deciduous forests LAI began to exhibit anomalies during less intense drought. The response thresholds of all other vegetation types were around the SPEI of −1.

4. Discussion

Previous studies commonly evaluated vegetation response to drought based on correlations between drought indices and vegetation indices. Such an approach however cannot capture the variety in response characteristics of vegetation. To more quantitatively assess the effects of drought on vegetation, we constructed a new framework. This framework is composed of drought indicator SPEI and a vegetation growth response indicator
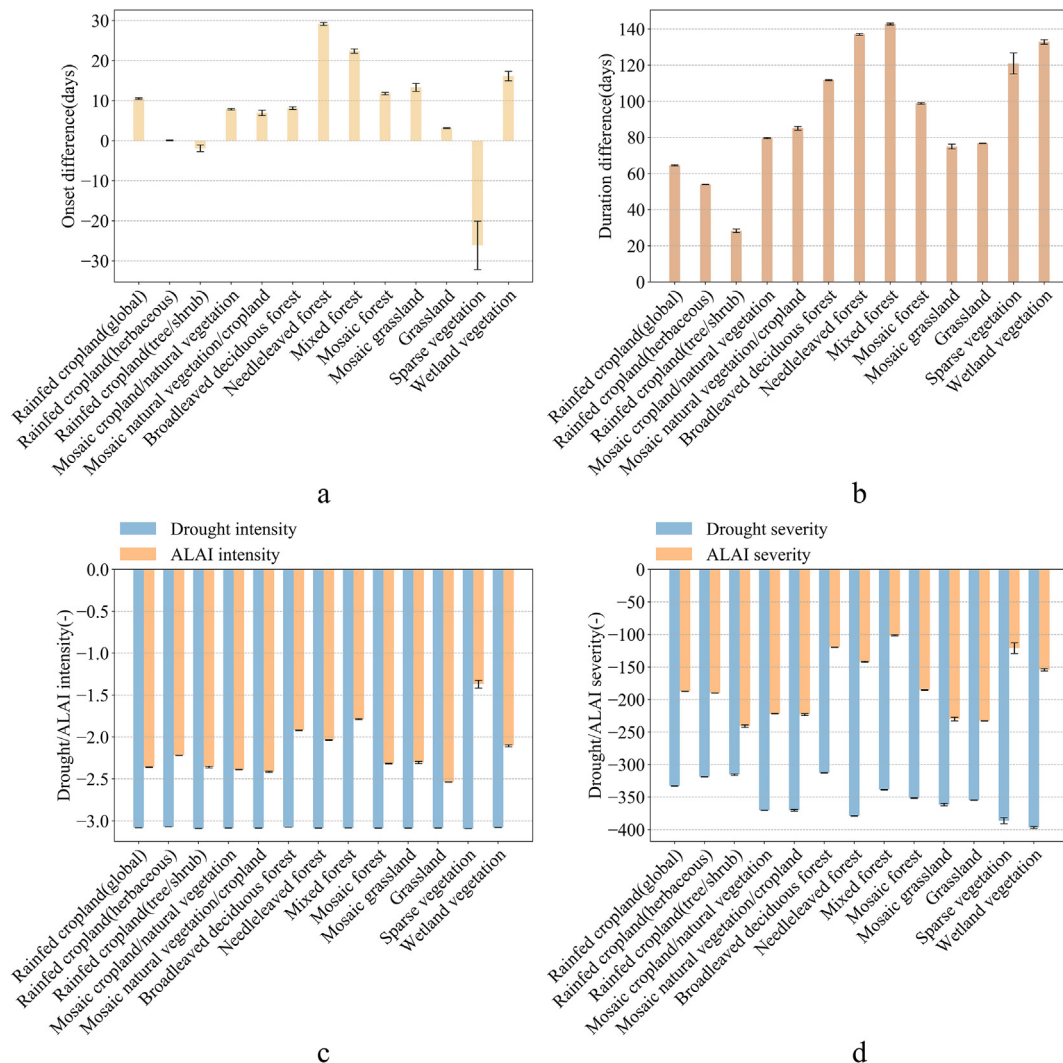
Fig. 4. Comparison of SPEI and anomaly LAI (ALAI) metrics. Panel a represents the difference between onsets by subtracting the onset of the longest drought event from the onset of the longest ALAI event. Panel b represents the difference between duration by subtracting ALAI duration from drought duration. Panels c-d represent drought and LAI intensity and severity for the different vegetation types, respectively.

based on the long-term anomaly in LAI. To account for the high spatiotemporal variation, particularly in vegetation responses, we established a high temporal and spatial resolution dataset to calculate both SPEI and ALAI. Based on these two indicators, we described the spatial and temporal characteristics from multiple perspectives, including onset, duration, intensity, and severity of both drought and its impacts.

4.1. Applying multi-metric framework to future water regulation

Application of our multi-metric framework provides all needed information on three aspects of vegetation responses to drought, including which vegetation types are sensitive, when will vegetation be damaged and how much will be the damage. Moreover, our framework provided an early warning threshold of vegetation damage by drought, which may aid in determining under which drought conditions it is necessary to take measures to mitigate the risk of negative drought impacts for a given vegetation type. These features will be helpful to future water regulation.

The different facets of vegetation responses reflect different component of vegetation strategies to deal with drought. For instance, we found that broadleaved deciduous forests responded faster and at milder drought conditions than other forest types. However, the severity of damage was not much different from other forest types. Their faster response at mild

drought conditions can be explained by their leaf shedding to protect the hydraulic system and leaf growth restrictions to balance production and survival under water stress (Schuldt, 2020)(Munné-Bosch and Alegre, 2004)(Marchin et al., 2010). Needleleaved forests showed the slowest response and only started to react under the severest drought conditions, but the damage they suffered is similar to that of broadleaved forests. Conifers tend to have a wider hydraulic safety margin (defined as differences between minimum xylem pressures and pressures that would cause hydraulic dysfunction) than angiosperms to avoid cavitation (Johnson et al., 2012) (Choat et al., 2012), with early stomatal closure and lower carbon gain (Carnicer et al., 2013)(Martínez-Ferri et al., 2000). This water saving strategy may explain their slow response to drought. Mixed forests also responded slowly to severe water stress, and the damage they suffered was low. Mixed forests may combine multiple strategies (tolerance, avoidance and recovery) to deal with drought which may increase their overall resistance (Pardos et al., 2021)(Mayoral et al., 2015) thanks to functional complementarity among coexisting tree species (Gazol and Camarero, 2016)(Loreau and de Mazancourt, 2013). In combination, our framework was able to pick up subtle differences in drought impacts of different forest types that were hard to distinguish previously (Carnicer et al., 2013).

Forests in natural ecosystems were less affected by drought stress than grasslands and croplands, which is consistent with results of previous
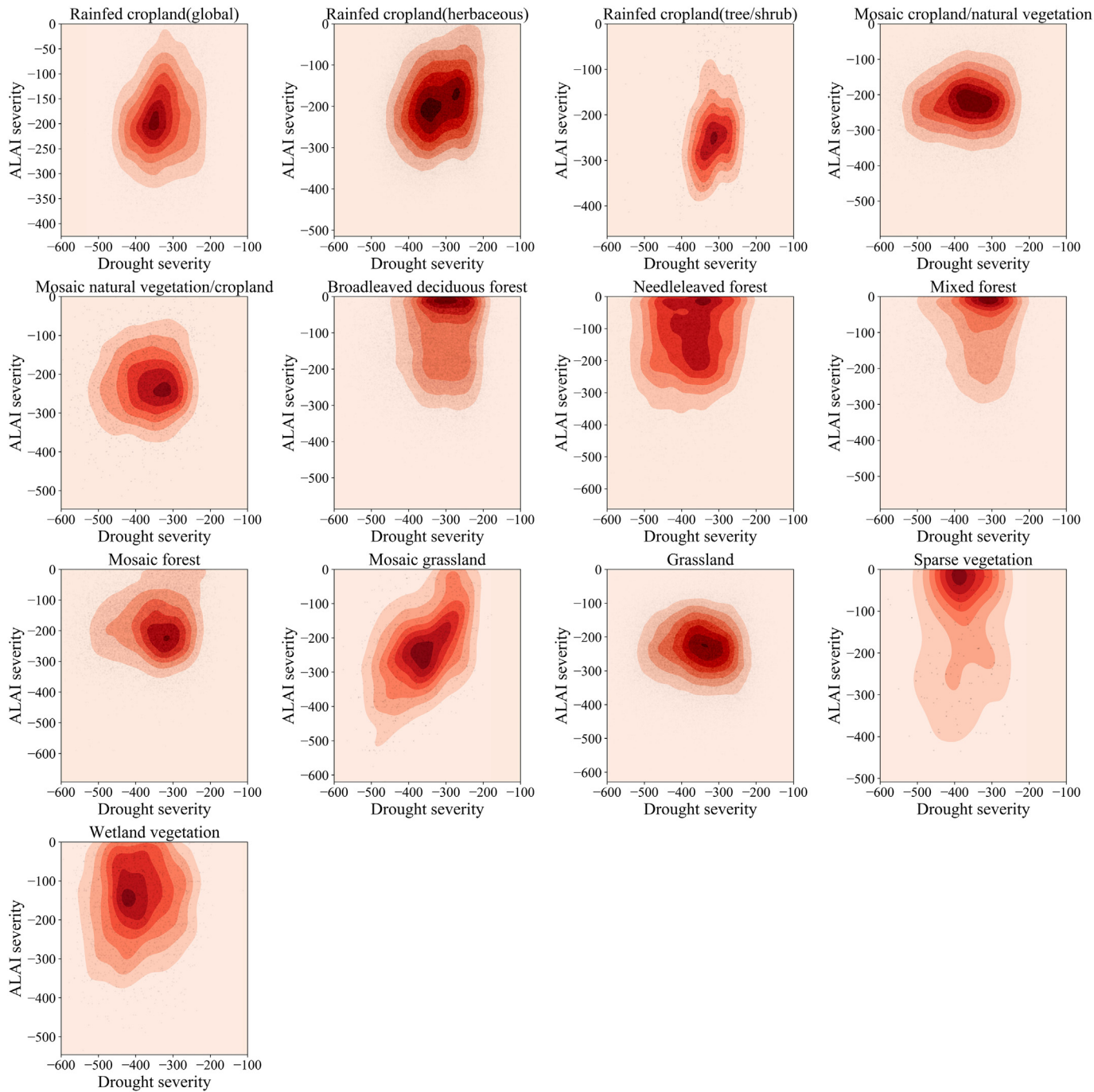
Fig. 5. Relationship between anomaly LAI (ALAI) severity and drought severity. The color represents the density of points as calculated based on Gaussian kernel density estimations (dark red: high density, light red: low density).

studies (Ding et al., 2020)(Nicolai-Shaw et al., 2017)(Xu, 2019). Our analysis showed that croplands and grasslands had a shorter delay at mild drought and experienced more severe damage despite irrigation practices in agricultural systems. Grasslands and croplands with shallow root systems can only absorb and utilize soil moisture from shallow layers, in which soil moisture responds to precipitation pulses quickly (Sala et al., 1992). In contrast, the well-developed deep roots of trees enable them to absorb water from deep soil layers, thus providing them with a certain buffer capacity during drought stress (Germon et al., 2020)(Nardini et al., 2016). However, we found that particular tree croplands (e.g. orchards) were highly sensitive to drought stress in agricultural ecosystems of this region, possibly related to the relatively shallow roots of the predominant crops in them

(Cockroft and Wallbrink, 1966). A quantitative understanding of these multi-faceted responses of vegetation can provide reliable guidance for future water management to mitigate drought impacts.

4.2. Vulnerability to drought for future drought impacts prediction

Our framework provided vulnerability estimates (Fig.5 and Fig.S6) based on the changes in the severity of vegetation impacts with increasing drought severity. These estimates express how vulnerability varies with drought, insights that a traditional correlation analysis does not provide. Our analysis shows that, with increasing drought severity, different vegetation types showed different increases in damage (Fig.5), probably related to
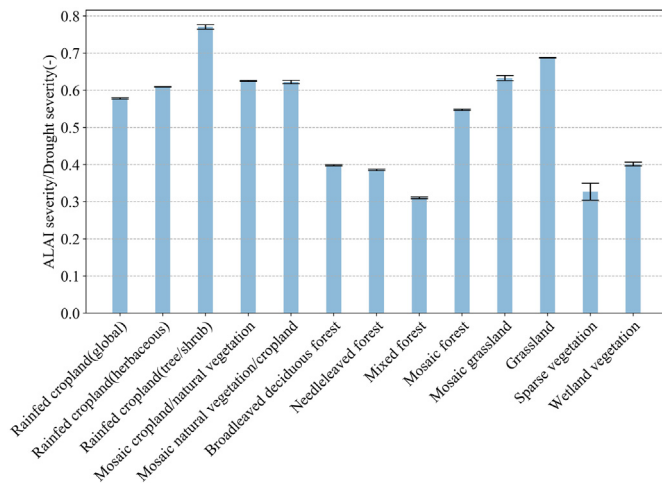
Fig. 6. The ratio of anomaly LAI (ALAI) to drought severity across 2018.

their different coping strategies (see Section 4.1). Particularly mosaic grasslands showed a large increase in damage with increasing drought severity, indicating that this vegetation type is highly susceptible to drought. The establishment and growth of woody seedlings is especially sensitive to drought (Van Wijk and Rodriguez-Iturbe, 2002)(Jeltsch et al., 2000), and the combination of seedlings and herbaceous plants likely explains the higher sensitivity of mosaic grasslands than other ecosystems. In contrast, mosaic forests (with a high proportion of woody plants) did not show a high sensitivity to drought. For ecosystems where crops are mixed with e.g. grasslands, forests, or shrubs, changes in the proportion of natural vegetation did not lead to very different responses to drought condition changing (e.g., compare the two mosaic cropland types).

The vulnerability analysis and the other analyses within our framework also show a large variation in responses within a vegetation type. This is likely due to variation in local environmental conditions, including differences in species composition, soil properties, groundwater availability and land management. Soil texture and groundwater levels vary in our study area with clayey and peat soils with shallow groundwater levels in the west and sandy soils with relatively deep groundwater levels in the east (Reijneveld et al., 2009). Both soil texture and groundwater levels are well-known to moderate drought impacts (e.g. Jiang et al., 2020). Also between vegetation types, differences in local environmental conditions probably play a role as groundwater levels and soil type likely also
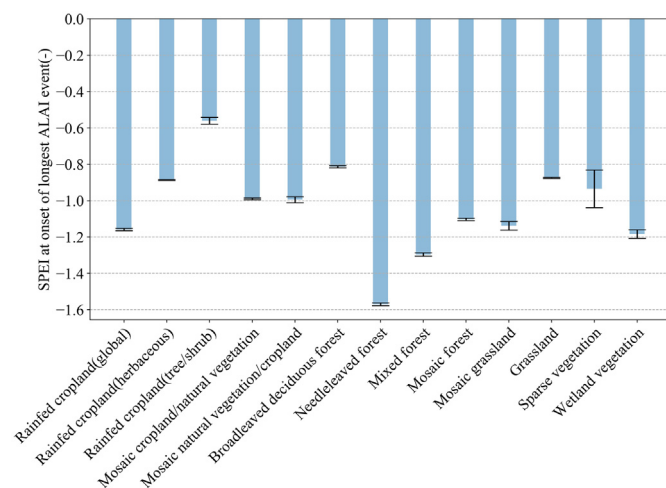
affect the spatial distribution of vegetation types, as related to the different strategies of vegetation types to deal with drought and other local environmental conditions. This implies that differences in sensitivities among vegetation types may express both the sensitivity itself as well as the moderation of those sensitivities by differences in the environmental conditions at which these vegetation types occur. Given that these effects are intrinsically coupled, they cannot be separated. Evaluations of future drought impacts should account for these variations within and between vegetation types and their causes to improve the quality of predictions.

4.3. Merits and limitations

In contrast to previous studies that mostly focused on one aspect of drought impacts, by combining different metrics, our framework comprehensively captures the temporal and spatial characteristics of drought effects. The observed patterns of the metrics within and between vegetation types have important implications for drought management as they give us an early warning signal of when ecosystems start to suffer damage. This allows taking measures at the appropriate drought conditions to maintain the stability of the ecosystem functioning and structure before drastic declines of vegetation canopy occur.

Similarly, our framework allows a more comprehensive evaluation of drought impacts across different ranges of drought severities. This has wide application potential for predicting future drought impacts in which droughts are likely to be more severe than in the current climate. Our framework indicates how vulnerabilities to drought will change and also which aspects of drought damage will be most affected in different vegetation types. Further research based on this framework would be helpful to evaluate the generality of the responses observed in this study.

While the high temporal and spatial resolution used in our framework is essential to properly quantify these patterns, this may also pose calculation restrictions when applied to larger extents. This is a limitation that needs to be accounted for. Moreover, the current analysis focussed on drought impacts during one year of drought. Legacy effect of droughts on ecosystem functioning in subsequent years (Anderegg et al., 2015)(Wu et al., 2018) was not taken into account. In principle though, our framework would allow for such explorations and quantifications of legacy effects. The application of this framework on a larger spatial scale and longer time sequences thus needs further explorations.

5. Conclusions

The 2018 drought had a major impact on vegetation growth in most regions of western Europe. We provide metrics to quantify spatial-temporal characteristics of SPEI and LAI based on the same criteria to calculate vegetation responses to drought across different vegetation types. This drought analysis framework facilitates a quantitative comparison and understanding of the intimate relationships between drought and its impacts on vegetation through multiple characteristics. The framework also allows revealing the variation in vulnerability to drought within and between vegetation types. Particularly the vulnerability assessment based on the relationship between drought severity and the severity of its corresponding vegetation damage allows differentiating different vegetation strategies in coping with increasing drought conditions. Our multiple metrics open a new internal perspective for drought impact evaluation, water management and future drought prediction studies.

Fig. 7. SPEI value at the start date of the longest LAI anomaly event in different vegetation types.

CRediT authorship contribution statement

Qi Chen: Conceptualization, Methodology, Investigation, Writing – original draft. **Joris Timmermans:** Conceptualization, Methodology, Writing – review & editing, Supervision. **Wen Wen:** Writing – review & editing. **Peter M. van Bodegom:** Conceptualization, Methodology, Writing – review & editing, Supervision.

Declaration of competing interest

Acknowledgements

Appendix A. Supplementary data

Supplementary data to this article can be found online at https://doi.org/10.1016/j.scitotenv.2022.154970.

References

Adams, J., 2017. climate_indices, An Open Source Python Library Providing Reference Implementations of Commonly Used Climate Indices.

Anderegg, W.R.L., Schwalm, C., Biondi, F., Camarero, J.J., Koch, G., Litvak, M., Ogle, K., Shaw, J.D., Shevliakova, E., Williams, A.P., Wolf, A., Ziaco, E., Pacala, S., 2015. Pervasive drought legacies in forest ecosystems and their implications for carbon cycle models. Science 80 (349), 528–532. https://doi.org/10.1126/SCIENCE.AAB1833/SUPPL_FILE/AAB1833-ANDEREGG-SM.PDF.

Bachmair, S., Tanguy, M., Hannaford, J., Stahl, K., 2018. How well do meteorological indicators represent agricultural and forest drought across Europe? Environ. Res. Lett. 13, 034042. https://doi.org/10.1088/1748-9326/AAAFDA.

Briffa, K.R., van der Schrier, G., Jones, P.D., 2009. Wet and dry summers in Europe since 1750: evidence of increasing drought. Int. J. Climatol. 29, 1894–1905. https://doi.org/10.1002/joc.1836.

Brito, S.S.B., Cunha, A.P.M.A., Cunningham, C.C., Alvalá, R.C., Marengo, J.A., Carvalho, M.A., 2018. Frequency, duration and severity of drought in the Semiarid Northeast Brazil region. Int. J. Climatol. 38, 517–529. https://doi.org/10.1002/JOC.5225.

Brown, M.E., 2008. Famine early warning systems and remote sensing data. Springer Science & Business Media.

Buitink, J., Swank, A.M., Van Der Ploeg, M., Smith, N.E., Benninga, H.J.F., Van Der Bolt, F., Carranza, C.D.U., Koren, G., Van der Velde, R., Teuling, A.J., 2020. Anatomy of the 2018 agricultural drought in the Netherlands using in situ soil moisture and satellite vegetation indices. Hydrol. Earth Syst. Sci. 24, 6021–6031. https://doi.org/10.5194/HESS-24-6021-2020.

C3S, 2019. Land cover classification gridded maps from 1992 to present derived from satellite observations. Available at: https://cds.climate.copernicus.eu/cdsapp#!/dataset/satellite-land-cover?tab=overview.

Camacho, F., Cernicharo, J., Lacaze, R., Baret, F., Weiss, M., 2013. GEOV1: LAI, FAPAR essential climate variables and FCOVER global time series capitalizing over existing products. Part 2: Validation and intercomparison with reference products. Remote Sens. Environ. 137, 310–329. https://doi.org/10.1016/j.rse.2013.02.030.

Carnicer, J., Barbeta, A., Sperlich, D., Coll, M., Penuelas, J., 2013. Contrasting trait syndromes in angiosperms and conifers are associated with different responses of tree growth to temperature on a large scale. Front. Plant Sci. 4. https://doi.org/10.3389/fpls.2013.00409.

Chen, J.M., Rich, P.M., Gower, S.T., Norman, J.M., Plummer, S., 1997. Leaf area index of boreal forests: Theory, techniques, and measurements. J. Geophys. Res. Atmos. 102, 29429–29443. https://doi.org/10.1029/97JD01107.

Chiang, F., Mazdiyasni, O., AghaKouchak, A., 2021. Evidence of anthropogenic impacts on global drought frequency, duration, and intensity. Nat. Commun. 121 (12), 1–10. https://doi.org/10.1038/s41467-021-22314-w.

Choat, B., Jansen, S., Brodribb, T.J., Cochard, H., Delzon, S., Bhaskar, R., Bucci, S.J., Feild, T.S., Gleason, S.M., Hacke, U.G., Jacobsen, A.L., Lens, F., Maherali, H., Martínez-Vilalta, J., Mayr, S., Mencuccini, M., Mitchell, P.J., Nardini, A., Pittermann, J., Pratt, R.B., Sperry, J.S., Westoby, M., Wright, I.J., Zanne, A.E., 2012. Global convergence in the vulnerability of forests to drought. Nat 2012 (4917426 491), 752–755. https://doi.org/10.1038/NATURE11688.

Ciais, P., Reichstein, M., Viovy, N., Granier, A., Ogée, J., Allard, V., Aubinet, M., Buchmann, N., Bernhofer, C., Carrara, A., Chevallier, F., De Noblet, N., Friend, A.D., Friedlingstein, P., Grünwald, T., Heinesch, B., Keronen, P., Knohl, A., Krinner, G., Loustau, D., Manca, G., Matteucci, G., Miglietta, F., Ourcival, J.M., Papale, D., Pilegaard, K., Rambal, S., Seufert, G., Soussana, J.F., Sanz, M.J., Schulze, E.D., Vesala, T., Valentini, R., 2005. Europe-wide reduction in primary productivity caused by the heat and drought in 2003. Nature 437, 529–533. https://doi.org/10.1038/nature03972.

Cockroft, B., Wallbrink, J.C., 1966. Root distribution of orchard trees. Aust. J. Agric. Res. 17, 49–54. https://doi.org/10.1071/AR9660049.

Copernicus Service Information, 2022. Leaf Area Index. Available at: https://land.copernicus.eu/global/products/lai.

Ding, Y., Xu, J., Wang, X., Peng, X., Cai, H., 2020. Spatial and temporal effects of drought on Chinese vegetation under different coverage levels. Sci. Total Environ. 716, 137166. https://doi.org/10.1016/j.scitotenv.2020.137166.

Fang, Y., Xiong, L., 2015. General mechanisms of drought response and their application in drought resistance improvement in plants. Cell. Mol. Life Sci. https://doi.org/10.1007/s00018-014-1767-0.

Field, C.B., Barros, V., Stocker, T.F., Dahe, Q., Jon Dokken, D., Ebi, K.L., Mastrandrea, M.D., Mach, K.J., Plattner, G.K., Allen, S.K., Tignor, M., Midgley, P.M., 2012. Managing the Risks of Extreme Events and Disasters to Advance Climate Change Adaptation: Special Report of the Intergovernmental Panel on Climate Change. Cambridge University Press https://doi.org/10.1017/CBO9781139177245.

Forner, A., Valladares, F., Aranda, I., 2018. Mediterranean trees coping with severe drought: Avoidance might not be safe. Environ. Exp. Bot. 155, 529–540. https://doi.org/10.1016/J.ENVEXPBOT.2018.08.006.

Garrigues, S., Allard, D., Baret, F., Weiss, M., 2006. Influence of landscape spatial heterogeneity on the non-linear estimation of leaf area index from moderate spatial resolution remote sensing data. Remote Sens. Environ. 105, 286–298. https://doi.org/10.1016/J.RSE.2006.07.013.

Gazol, A., Camarero, J.J., 2016. Functional diversity enhances silver fir growth resilience to an extreme drought. J. Ecol. 104, 1063–1075. https://doi.org/10.1111/1365-2745.12575.

Gebremeskel Haile, G., Tang, Q., Leng, G., Jia, G., Wang, J., Cai, D., Sun, S., Baniya, B., Zhang, Q., 2020. Long-term spatiotemporal variation of drought patterns over the Greater Horn of Africa. Sci. Total Environ. 704, 135299. https://doi.org/10.1016/J.SCITOTENV.2019.135299.

Germon, A., Laclau, J.P., Robin, A., Jourdan, C., 2020. Tamm Review: deep fine roots in forest ecosystems: Why dig deeper? For. Ecol. Manag. https://doi.org/10.1016/j.foreco.2020.118135.

Gouveia, C.M., Trigo, R.M., Beguería, S., Vicente-Serrano, S.M., 2017. Drought impacts on vegetation activity in the Mediterranean region: an assessment using remote sensing data and multi-scale drought indicators. Glob. Planet. Chang. 151, 15–27. https://doi.org/10.1016/j.gloplacha.2016.06.011.

Gower, S.T., Norman, J.M., 1991. Rapid estimation of leaf area index in conifer and broad-leaf plantations. Ecology 72, 1896–1900. https://doi.org/10.2307/1940988.

Grillakis, M.G., 2019. Increase in severe and extreme soil moisture droughts for Europe under climate change. Sci. Total Environ. 660, 1245–1255. https://doi.org/10.1016/j.scitotenv.2019.01.001.

Huete, A., Didan, K., Miura, T., Rodriguez, E.P., Gao, X., Ferreira, L.G., 2002. Overview of the radiometric and biophysical performance of the MODIS vegetation indices. Remote Sens. Environ. 83, 195–213. https://doi.org/10.1016/S0034-4257(02)00096-2.

Ivits, E., Horion, S., Erhard, M., Fensholt, R., 2016. Assessing European ecosystem stability to drought in the vegetation growing season. Glob. Ecol. Biogeogr. 25, 1131–1143. https://doi.org/10.1111/geb.12472.

Jamro, S., Channa, F.N., Dars, G.H., Ansari, K., Krakauer, N.Y., 2020. Exploring the evolution of drought characteristics in Balochistan, Pakistan. Appl. Sci. 10, 913. https://doi.org/10.3390/app10030913.

Jeltsch, F., Weber, G.E., Grimm, V., 2000. Ecological buffering mechanisms in savannas: a unifying theory of long-term tree-grass coexistence. Plant Ecol. 161, 161–171.

Ji, L., Peters, A.J., 2003. Assessing vegetation response to drought in the northern Great Plains using vegetation and drought indices. Remote Sens. Environ. 87, 85–98. https://doi.org/10.1016/S0034-4257(03)00174-3.

Jiang, P., Ding, W., Yuan, Y., Ye, W., 2020. Diverse response of vegetation growth to multi-time-scale drought under different soil textures in China's pastoral areas. J. Environ. Manag. 274, 110992. https://doi.org/10.1016/J.JENVMAN.2020.110992.

Johnson, D.M., McCulloh, K.A., Woodruff, D.R., Meinzer, F.C., 2012. Hydraulic safety margins and embolism reversal in stems and leaves: Why are conifers and angiosperms so different? Plant Sci. 195, 48–53. https://doi.org/10.1016/J.PLANTSCI.2012.06.010.

Khabbazan, S., Vermunt, P., Steele-Dunne, S., Arntz, L.R., Marinetti, C., van der Valk, D., Iannini, L., Molijn, R., Westerdijk, K., van der Sande, C., 2019. Crop monitoring using sentinel-1 data: a case study from the Netherlands. Remote Sens. 11, 1887. https://doi.org/10.3390/RS11161887.

Kogan, F.N., 1995b. Application of vegetation index and brightness temperature for drought detection. Adv. Sp. Res. 15, 91–100. https://doi.org/10.1016/0273-1177(95)00079-T.

Kogan, F.N., 1997. Global drought watch from space. Bull. Am. Meteorol. Soc. 78, 621–636. https://doi.org/10.1175/1520-0477(1997)078<0621:gdwfs>2.0.co;2.

Kogan, Felix N., 1995a. Droughts of the late 1980s in the United States as derived from NOAA polar-orbiting satellite data. Bull. Am. Meteorol. Soc. 76, 655–668. https://doi.org/10.1175/1520-0477(1995)076<0655:dotlit>2.0.co;2.

Larcher, W., 2003. Physiological Plant Ecology: Ecophysiology and Stress Physiology of Functional Groups. Springer Science & Business Media.

Loreau, M., de Mazancourt, C., 2013. Biodiversity and ecosystem stability: a synthesis of underlying mechanisms. Ecol. Lett. 16, 106–115. https://doi.org/10.1111/ELE.12073.

Marchin, R., Zeng, H., Hoffmann, W., 2010. Drought-deciduous behavior reduces nutrient losses from temperate deciduous trees under severe drought. Oecologia 163, 845–854. https://doi.org/10.1007/s00442-010-1614-4.

Martínez-Ferri, E., Balaguer, L., Valladares, F., Chico, J.M., Manrique, E., 2000. Energy dissipation in drought-avoiding and drought-tolerant tree species at midday during the Mediterranean summer. Tree Physiol. 20, 131–138. https://doi.org/10.1093/TREEPHYS/20.2.131.

Mayoral, C., Calama, R., Sánchez-González, M., Pardos, M., 2015. Modelling the influence of light, water and temperature on photosynthesis in young trees of mixed Mediterranean forests. New For. 46, 485–506. https://doi.org/10.1007/S11056-015-9471-Y/FIGURES/7.

McKee, T.B., D, N.J., K, J., 1993. The relation of drought frequency and duration to time scales. Proceedings of the Eighth Conference on Applied Climatology. American Meteorological Society, Boston, pp. 179–184.

Mishra, A.K., Singh, V.P., 2010. A review of drought concepts. J. Hydrol. https://doi.org/10.1016/j.jhydrol.2010.07.012.

Munné-Bosch, S., Alegre, L., 2004. Die and live: leaf senescence contributes to plant survival under drought stress. Funct. Plant Biol. https://doi.org/10.1071/FP03236.

Nardini, A., Casolo, V., Dal Borgo, A., Savi, T., Stenni, B., Bertoncin, P., Zini, L., Mcdowell, N.G., 2016. Rooting depth, water relations and non-structural carbohydrate dynamics in three woody angiosperms differentially affected by an extreme summer drought. Plant Cell Environ. 39, 618–627. https://doi.org/10.1111/pce.12646.

Nicolai-Shaw, N., Zscheischler, J., Hirschi, M., Gudmundsson, L., Seneviratne, S.I., 2017. A drought event composite analysis using satellite remote-sensing based soil moisture. Remote Sens. Environ. 203, 216–225. https://doi.org/10.1016/j.rse.2017.06.014.

Palmer, W.C., 1965. Meteorological Drought. 45. U.S. Weather Bur. Res. Pap.

Pardos, M., del Río, M., Pretzsch, H., Jactel, H., Bielak, K., Bravo, F., Brazaitis, G., Defossez, E., Engel, M., Godvod, K., Jacobs, K., Jansone, L., Jansons, A., Morin, X., Nothdurft, A., Oreti, L., Ponette, Q., Pach, M., Riofrío, J., Ruíz-Peinado, R., Tomao, A., Uhl, E., Calama, R., 2021. The greater resilience of mixed forests to drought mainly depends on their composition: analysis along a climate gradient across Europe. For. Ecol. Manag. 481, 118687. https://doi.org/10.1016/J.FORECO.2020.118687.

Páscoa, P., Gouveia, C.M., Russo, A.C., Bojariu, R., Vicente-Serrano, S.M., Trigo, R.M., 2018. Vegetation vulnerability to drought on southeastern Europe. Hydrol. Earth Syst. Sci. Discuss. 2018, 1–29. https://doi.org/10.5194/hess-2018-264.

Philip, S.Y., Kew, S.F., Van Der Wiel, K., Wanders, N., Jan Van Oldenborgh, G., Philip, S.Y., 2020. Regional differentiation in climate change induced drought trends in the Netherlands. Environ. Res. Lett. 15, 094081. https://doi.org/10.1088/1748-9326/AB97CA.

Reijneveld, A., van Wensem, J., Oenema, O., 2009. Soil organic carbon contents of agricultural land in the Netherlands between 1984 and 2004. Geoderma 152, 231–238. https://doi.org/10.1016/J.GEODERMA.2009.06.007.

Rita, A., Camarero, J.J., Nolè, A., Borghetti, M., Brunetti, M., Pergola, N., Serio, C., Vicente-Serrano, S.M., Tramutoli, V., Ripullone, F., 2020. The impact of drought spells on forests depends on site conditions: the case of 2017 summer heat wave in southern Europe. Glob. Chang. Biol. 26, 851–863. https://doi.org/10.1111/GCB.14825.

Roebeling, R.A., Holleman, I., 2009. SEVIRI rainfall retrieval and validation using weather radar observations. J. Geophys. Res. 114, D21202. https://doi.org/10.1029/2009JD012102.

Roebeling, R.A., Feijt, A.J., Stammes, P., 2006. Cloud property retrievals for climate monitoring: Implications of differences between Spinning Enhanced Visible and Infrared Imager (SEVIRI) on METEOSAT-8 and Advanced Very High Resolution Radiometer (AVHRR) on NOAA-17. J. Geophys. Res. Atmos. 111. https://doi.org/10.1029/2005JD006990.

Running, S., Mu, Q., Zhao, M., 2017. MOD16A2 MODIS/Terra Net Evapotranspiration 8-Day L4 Global 500m SIN Grid V006 NASA EOSDIS Land Processes DAAC NASA EOSDIS Land Processes DAAC. https://doi.org/10.5067/MODIS/MOD16A2.006.

Ruosteenoja, K., Markkanen, T., Venäläinen, A., Räisänen, P., Peltola, H., 2018. Seasonal soil moisture and drought occurrence in Europe in CMIP5 projections for the 21st century. Clim. Dyn. 50, 1177–1192. https://doi.org/10.1007/s00382-017-3671-4.

Saatchi, S., Asefi-Najafabady, S., Malhi, Y., Aragão, L.E.O.C., Anderson, L.O., Myneni, R.B., Nemani, R., 2013. Persistent effects of a severe drought on Amazonian forest canopy. Proc. Natl. Acad. Sci. U. S. A. 110, 565–570. https://doi.org/10.1073/PNAS.1204651110/-/DCSUPPLEMENTAL.

Sala, O.E., Lauenroth, W.K., Parton, W.J., 1992. Long-term soil water dynamics in the shortgrass steppe. Ecology 73, 1175–1181. https://doi.org/10.2307/1940667.

Schuldt, B., 2020. A first assessment of the impact of the extreme 2018 summer drought on Central European forests. Basic Appl. Ecol https://doi.org/10.1016/j.baae.2020.04.003.

Semenov, M.A., Shewry, P.R., 2011. Modelling predicts that heat stress, not drought, will increase vulnerability of wheat in Europe. Sci. Rep. 1, 1–5. https://doi.org/10.1038/srep00066.

Sepulcre-Canto, G., Horion, S., Singleton, A., Carrao, H., Vogt, J., 2012. Development of a combined drought indicator to detect agricultural drought in Europe. Nat. Hazards Earth Syst. Sci. 12, 3519–3531. https://doi.org/10.5194/NHESS-12-3519-2012.

Spinoni, J., Vogt, J.V., Naumann, G., Barbosa, P., Dosio, A., 2018. Will drought events become more frequent and severe in Europe? Int. J. Climatol. 38, 1718–1736. https://doi.org/10.1002/joc.5291.

Sun, Q., Miao, C., Duan, Q., Ashouri, H., Sorooshian, S., Hsu, K.L., 2018. A review of global precipitation data sets: data sources, estimation, and intercomparisons. Rev. Geophys. 56, 79–107. https://doi.org/10.1002/2017RG000574.

Tang, H., Brolly, M., Zhao, F., Strahler, A.H., Schaaf, C.L., Ganguly, S., Zhang, G., Dubayah, R., 2014. Deriving and validating Leaf Area Index (LAI) at multiple spatial scales through lidar remote sensing: a case study in Sierra National Forest. CA. Remote Sens. Environ. 143, 131–141. https://doi.org/10.1016/J.RSE.2013.12.007.

Toreti, A., 2014. Gridded agro-meteorological data in Europe. European Commission, Joint Research Centre (JRC) [Dataset] PID: http://data.europa.eu/89h/jrc-marsop4-7-weather_obs_grid_2019.

Van Wijk, M.T., Rodriguez-Iturbe, I., 2002. Tree-grass competition in space and time: Insights from a simple cellular automata model based on ecohydrological dynamics. Water Resour. Res. 38, 1–18. https://doi.org/10.1029/2001WR000768.

Verger, A., Baret, F., Weiss, M., 2014. Near real-time vegetation monitoring at global scale. IEEE J. Sel. Top. Appl. Earth Obs. Remote Sens. 7, 3473–3481. https://doi.org/10.1109/JSTARS.2014.2328632.

Vicente-Serrano, S.M., Beguería, S., López-Moreno, J.I., 2010. A multiscalar drought index sensitive to global warming: The standardized precipitation evapotranspiration index. J. Clim. 23, 1696–1718. https://doi.org/10.1175/2009JCLI2909.1.

Vicente-Serrano, S.M., Gouveia, C., Camarero, J.J., Beguería, S., Trigo, R., López-Moreno, J.I., Azorín-Molina, C., Pasho, E., Lorenzo-Lacruz, J., Revuelto, J., Morán-Tejeda, E., Sanchez-Lorenzo, A., 2013. Response of vegetation to drought time-scales across global land biomes. Proc. Natl. Acad. Sci. U. S. A. 110, 52–57. https://doi.org/10.1073/pnas.1207068110.

Vicente-Serrano, S.M., Lopez-Moreno, J.I., Beguería, S., Lorenzo-Lacruz, J., Sanchez-Lorenzo, A., García-Ruiz, J.M., Azorin-Molina, C., Morán-Tejeda, E., Revuelto, J., Trigo, R., Coelho, F., Espejo, F., 2014. Evidence of increasing drought severity caused by temperature rise in southern Europe. Environ. Res. Lett. 9, 044001. https://doi.org/10.1088/1748-9326/9/4/044001.

Volaire, F., 2018. A unified framework of plant adaptive strategies to drought: crossing scales and disciplines. Glob. Chang. Biol. 24, 2929–2938. https://doi.org/10.1111/GCB.14062.

Wang, Q., Shi, P., Lei, T., Geng, G., Liu, J., Mo, X., Li, X., Zhou, H., Wu, J., 2015. The alleviating trend of drought in the Huang-Huai-Hai Plain of China based on the daily SPEI. Int. J. Climatol. 35, 3760–3769. https://doi.org/10.1002/joc.4244.

Wu, X., Liu, H., Li, X., Ciais, P., Babst, F., Guo, W., Zhang, C., Magliulo, V., Pavelka, M., Liu, S., Huang, Y., Wang, P., Shi, C., Ma, Y., 2018. Differentiating drought legacy effects on vegetation growth over the temperate Northern Hemisphere. Glob. Chang. Biol. 24, 504–516. https://doi.org/10.1111/GCB.13920.

Xu, H. Jie, Wang, X. Ping, Zhao, C. Yan, Zhang, X. Xiao, 2019. Responses of ecosystem water use efficiency to meteorological drought under different biomes and drought magnitudes in northern China. Agric. For. Meteorol. 278, 107660. https://doi.org/10.1016/J.AGRFORMET.2019.107660.

Yao, N., Li, L., Feng, P., Feng, H., Li Liu, D., Liu, Y., Jiang, K., Hu, X., Li, Y., 2020. Projections of drought characteristics in China based on a standardized precipitation and evapotranspiration index and multiple GCMs. Sci. Total Environ. 704, 135245. https://doi.org/10.1016/J.SCITOTENV.2019.135245.

Zhang, Q., Kong, D., Singh, V.P., Shi, P., 2017. Response of vegetation to different time-scales drought across China: spatiotemporal patterns, causes and implications. Glob. Planet. Chang. 152, 1–11. https://doi.org/10.1016/j.gloplacha.2017.02.008.

Zhao, A., Zhang, A., Cao, S., Liu, X., Liu, J., Cheng, D., 2018. Responses of vegetation productivity to multi-scale drought in Loess Plateau, China. Catena 163, 165–171. https://doi.org/10.1016/j.catena.2017.12.016.